Chemical Engineering Journal 155 (2009) 941–949

Contents lists available at ScienceDirect

Chemical Engineering Journal

journal homepage: www.elsevier.com/locate/cej

Hydrogenation of sunflower oil over different palladium supported catalysts: Activity and selectivity

María B. Fernández, Jhon F. Sánchez M., Gabriela M. Tonetto*, Daniel E. Damiani

PLAPIQUI (UNS-CONICET), Camino La Carrindanga Km 7, CC 717, CP 8000, Bahía Blanca, Argentina

ARTICLE INFO

Article history:
Received 2 April 2009
Received in revised form
10 September 2009
Accepted 22 September 2009

Keywords:
Hydrogenation
Isomerization
Palladium
Sunflower oil
Trans-isomers

ABSTRACT

Six palladium catalysts were prepared using different precursors (palladium acetylacetonate, palladium nitrate and tetraamminepalladium nitrate) and supports (α-Al_2O_3, γ-Al_2O_3, ZSM-5, and MCM-22). The samples were characterized by atomic absorption spectroscopy, N_2 adsorption isotherms, XRD, H_2 chemisorption, transmission electron microscopy and temperature programmed reduction. The activity and selectivity of the catalysts were investigated in the hydrogenation of sunflower oil and compared to a commercial Ni catalyst.

Pd catalysts showed a higher activity, similar *trans*-isomer formation, and were more selective towards monoene formation than Ni catalysts. On the other hand, under the studied operating conditions, the different supports did not improve significantly the selectivity or the activity of the reaction.

The γ-alumina supported Pd catalyst, with a metal loading of 0.78 wt% and a 60% dispersion, showed a specific activity higher than the other Pd catalysts. For the same double bond conversion, this sample originated a slightly lower amount of total *trans*-isomers than the Ni catalyst, but it produced less saturated compound and was more selective towards monounsaturated fatty acid formation.

1. Introduction

The hydrogenation of vegetable oils is an important practice in the modification of fats and oils. The general purpose of this process is to increase the melting point and to improve the oxidation properties of the liquid oil [1]. The process was patented in 1903 and first commercialized by Procter & Gamble in 1911. During World War II, butter was subject to rationing, and the use of margarine and vegetable shortenings rapidly increased.

The chemistry of the hydrogenation processing of oils involved three simultaneous reactions: saturation of double bonds, and geometric (*cis–trans*) and positional isomerizations. The quality and physical properties of the hydrogenated oil are greatly influenced by the number of double bonds present and the *cis–trans*-isomers of fatty acids. The *trans*-fatty acids (TFA) have been reported to be unfavorable to human diet due to undesirable health effects. It has been demonstrated that the percentage of TFA contained in the diet is strongly correlated with coronary heart diseases [2,3].

Other aspect that it is gaining importance is the use of vegetable oils for non-food applications, such as lubricants [4,5]. Most lubricants are made from mineral oil, and although bio-lubricants are more expensive, vegetable oils show many advantages. They have low-toxicity, are biodegradable and present lower evaporation rates (up to 20% less than mineral oils). Vegetable oils used as lubricants need a higher viscosity, and to be resistant to oxidative rancidity and hydrolysis; for that reason, the partial hydrogenation of the oil is necessary.

Industrially, hydrogenation is performed in batch slurry reactors at temperatures of the order of 150–225 °C, and pressures ranging between 69 and 413 kPa in the presence of a supported or Raney Ni catalyst.

It is known that higher temperatures and lower pressures result in higher TFA levels [6]. Nevertheless, in common industrial hydrogenation processes it has not been possible to produce partially hydrogenated oil with a low *trans*-isomer content.

Several alternatives to conventional hydrogenation have been proposed in the past few years. Most of them describe new catalyst development and modification, especially palladium [5,7,8]. The use of Pd catalysts in the hydrogenation of edible oils is attractive due to their higher activity than Ni, and because the operation can be carried out under softer conditions.

Nohair et al. [5] studied the selective hydrogenation of ethyl esters of sunflower oil (SOEE) in the presence of supported Pd catalysts at low temperature (40 °C) in ethanol as solvent. Under these conditions, the authors found that the SOEE hydrogenation reaction was insensitive to the size of the Pd particles deposited on silica. The use of various oxide supports (α-Al_2O_3, γ-Al_2O_3, TiO_2, MgO, ZnO, CeO_2, $CeZrO_2$) did not improve the *cis*-C18:1 selectivity in the Pd catalyst.

* Corresponding author. Tel.: +54 291 4861700; fax: +54 291 4861600.
E-mail address: gtonetto@plapiqui.edu.ar (G.M. Tonetto).

1385-8947/$ – see front matter © 2009 Elsevier B.V. All rights reserved.
doi:10.1016/j.cej.2009.09.037

Plourde et al. [8] studied the hydrogenation of sunflower and canola oils over a silica supported palladium catalyst. Their best activity and selectivity results were found for catalyst supports with a pore diameter between 7 and 8 nm and a Pd content in the concentration range of 0.8–1.2 wt%.

A previous study was performed in our laboratory on the subject of alumina supported Pd–Me (Me = Mo, V and Pb) catalysts in sunflower oil hydrogenation [9]. A theoretical study was also carried out using molecular mechanics (MM2) and extended Hückel to analyze the hydrogenation and *cis*/*trans* isomerization mechanisms of the oleic fatty acid [10].

The aim of the present study is to explore the effects of metal particle size and supports on the activity and selectivity of Pd catalysts in the partial hydrogenation of sunflower oil. A comparative evaluation of the performance of Pd catalysts and a commercial Ni catalyst was performed.

2. Materials and methods

2.1. Sample preparation

Pd/α(A) and Pd/γ(A) catalysts were prepared by wet impregnation of the support: γ-Al_2O_3 (Condea, Puralox) and α-Al_2O_3 (Rhone Poulenc) with a solution of $Pd(C_5H_7O_2)_2$ (Alpha) in benzene. The support materials were impregnated with a volume of solution equal to five times the pore volume of the support. They were in contact for 72 h at 25 °C. After that, the catalysts were dried in N_2 at 150 °C for 2 h, and then calcined in chromatographic air at 500 °C for 2 h.

The Pd/α(N) and Pd/γ(N) catalysts were prepared by impregnation of α- and γ-Al_2O_3 respectively with $Pd(NO_3)_2$ using the incipient wetness method. The metal precursor was dissolved in a volume of bi-distillated water equal to the pore volume of the support (pH = 9). The impregnated supports were dried at room temperature for 24 h. The catalysts were calcined in chromatographic air at 500 °C for 2 h.

Prior to impregnation, the different supports were dried under N_2 flow at 150 °C for 2 h.

In order to transform the Na-zeolites into their acid forms, both NaZSM-5 (Chemie Uetikon AG) and NaMCM-22 (kindly provided by Prof. Sibele Pergher) zeolites were transformed into ammonium form by ion exchange with 1 M NH_4Cl solution at 80 °C for 6 h under stirring conditions. This operation was followed by filtration and three water washings. The zeolite samples were dried in air at 90 °C for 4 h, and at 120 °C for 6 h, and calcined in chromatographic air at 500 °C for 4 h.

Once the ion exchange operation was completed, the zeolitic supports were impregnated using the incipient wetness method, with $[Pd(NH_3)_4](NO_3)_2$ as metal precursor. The catalysts were dried and calcined at 300 °C. These samples are referred to as Pd/ZSM-5 and Pd/MCM-22.

The concentration of the impregnating solutions was adjusted to obtain a Pd loading of 1 wt% in the six prepared catalysts.

2.2. Catalyst characterization

The metal content was determined by atomic absorption spectrometry (AAS, Instrumentation Laboratory 551), using an air–acetylene burner and a Pd hollow-cathode lamp unit.

In order to measure the specific surface area, pore size and pore volume in bare supports and catalyts, N_2 adsorption isotherms were performed on a volumetric system Nova 1200e Quantachrome Instruments, using nitrogen as adsorbing gas at −196 °C. Prior to adsorption, the supports and catalysts were outgassed for 3 h at 300 °C. BET isotherm equation for macroporous and mesoporous solids, Langmuir equation for microporous solids, and t-plot equations were used for the evaluation of the specific (internal and external) surface areas. The pore size distribution for mesopore solids was determined using the BJH method [11], and for microporous solids the Horvath–Kawazoe approach [12] with the correction proposed by Cheng and Yang [13]. Table 1 reports the values of the physical properties of the adsorbate and adsorbents used in the micropore size distribution calculations.

Table 1
Values of the physical properties used in micropore size distribution calculations.

Parameter	Adsorbent: zeolite	Adsorbate: N_2
Diameter (nm)	0.276	0.3
Polarizability (cm^3/mol)	2.5×10^{-24}	1.46×10^{-24}
Magnetic susceptibility (cm^3/mol)	1.3×10^{-29}	2.0×10^{-29}
Density per unit area (mol/cm^2)	1.0×10^{15}	6.7×10^{14}

XRD patterns were collected using the powder method in a Rigaku diffractometer equipped with Cu Kα X-ray source and a Ni filter operated at 35 kV and 15 mA.

Hydrogen chemisorption runs were carried out in a conventional pulse apparatus [14] at atmospheric pressure and 100 °C. Prior to chemisorption, the catalysts were reduced *in situ* at 300 °C in flowing H_2. The fraction of exposed Pd was calculated assuming that one hydrogen atom is adsorbed per surface Pd metal atom.

The particle size distribution was determined by transmission electron microscopy (TEM), using a Joel 100 CX instrument operated at 100 kV. The Pd catalysts were ground and dispersed onto holey carbon-coated Cu grids for direct observation.

Temperature programmed reduction (TPR) experiments were performed in a conventional apparatus, as described in [15]. Before reduction, the catalyst (∼40 mg) was oxidized in flowing chromatographic air at 300 °C for 1 h, and purged and cooled in Ar. A mixture of 5% H_2 in Ar flow was then passed through the sample, and the temperature raised from −50 °C to 350 °C at a heating rate of 10 °C min^{-1}.

2.3. Catalytic test

Hydrogenation tests were carried out in a flat-bottom, 0.064 m diameter, 600 cm^3 Parr reactor, operated in a semi-continue mode. The reactor was connected to a hydrogen source (AGA chromatographic grade) maintained at constant pressure. H_2 consumption was measured during the reaction.

The catalytic tests were performed at 100 °C and 413.5 kPa for 1 h, using 250 cm^3 of commercial refined sunflower oil. The fatty acid composition and properties of the refined sunflower oil used are given in Table 5. The reduced catalyst was added to the reactor (containing the sunflower oil at reaction temperature). Then, the pressure was increased in order to start the reaction.

A commercial Ni/SiO_2 catalyst was used as a reference (Pricat 9910: 22% Ni, 4% SiO_2 dispersed in hydrogenated edible fats). The hydrogenation was performed at 180 °C with 0.23% Ni catalyst. That temperature was selected to reproduce similar industrial operating conditions. The Pd catalyst weight was adjusted in order to keep the weight of exposed Pd constant along the various experiments (see Table 5).

The analytical studies were carried out with an AGILENT 4890D gas chromatograph (GC) equipped with a flame ionization detector (FID), following the procedures established by the AOCS Ce 1c-89 norm. A 100 m long SUPELCO 2560 capillary column, with a nominal diameter of 0.25 mm and a nominal film thickness of 0.20 mm, was used for the separation of the different compounds present in the samples. The iodine number (IV) was calculated from the fatty acid composition following the AOCS Cd 1c-85 norm.

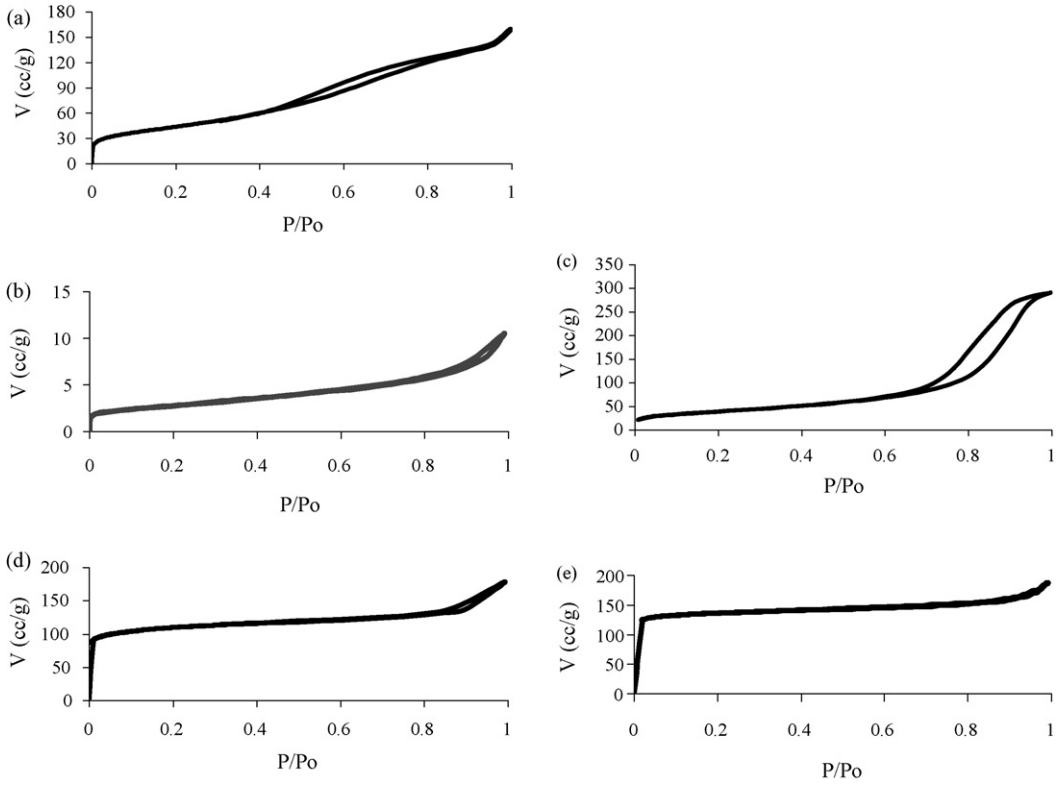

Fig. 1. Nitrogen adsorption–desorption isotherms for (a) Ni–SiO_2, (b) α-Al_2O_3, (c) γ-Al_2O_3, (d) ZSM-5, and (e) MCM-22.

Because hydrogenation of edible oils is a three-phase process, several transport limitations may occur. The volumetric gas–liquid mass-transfer coefficient (K_La) was separately measured using an excess of catalyst load [16]. Intraparticle diffusion limitations for hydrogen were estimated with the Weisz–Prater criterion [17].

3. Results and discussion

3.1. Catalyst preparation and characterization

3.1.1. Supports

Textural characterization of the supports, namely specific surface area, pore size and pore size distribution, was studied by analysis of nitrogen isotherms (at −196 °C) and by numerical treatment of the adsorption data.

Fig. 1 reports the nitrogen adsorption–desorption isotherms of all the samples. The shape of the adsorption isotherms of ZSM-5 and MCM-22 is Type I in the Brunauer, Deming, Deming and Teller [18] classification, typical of microporous solids. N_2 isotherms of Ni–SiO_2 and γ-alumina are Type IV, corresponding to a mesoporous structure. In addition, the hysteresis loop of these two samples seems to be of type H3 IUPAC classification, which is associated with porous solid having slip-shape pores. The isotherm of α-Al_2O_3 is Type II, indicating a macroporous solid. The small hysteresis loop is in agreement with the small internal area reported in Table 2.

Fig. 2 presents the pore size distribution (PSD) obtained from the adsorption data. The microporous solids (ZSM5 and MCM-22) showed a main pore diameter of 4.5 and 5.7 Å, respectively. Both values are in agreement with the reported average pore diameter for these materials. In the case of Ni–SiO_2 and γ-alumina, the pore diameter was 43.6 and 97.7 Å, respectively.

Table 2 reports the specific (internal and external) surface areas and pore volume of the supports used.

3.1.2. Catalysts

Table 3 lists the catalysts and their main properties.

When $Pd(C_5H_7O_2)_2$ was used as precursor, the metal loading was higher on γ-Al_2O_3 than on α-Al_2O_3 (0.78 and 0.65, respectively). This would be a consequence of the lower OH concentration on α-Al_2O_3, because the acetylacetonate ($Pd(Acac)_2$) anchoring over the alumina surface takes place through a mechanism of ligand

Table 2
Textural properties of supports.

Sample	ISA (m^2/g)	ESA (m^2/g)	Average pore diameter (Å)	Pore volume (cm^3/g)
ZSM-5	307.2	66.3	4.5	0.27
MCM-22	379.7	49.6	5.7	0.29
α-Al_2O_3	0.4	8.8	–	0.47
Ni–SiO_2	–	160.6	43.6	0.24
γ-Al_2O_3	–	134.4	97.7	0.43

ESA: external surface area.
ISA: internal surface area.
(–) Not detectable.

Table 3
Catalyst characterization: metal loading, palladium dispersion and palladium particle size.

Catalyst	Pd (wt%)	Pd_S/Pd_T (%)[a]	d (nm)[b]	d (nm)[c] TEM	BET (m^2/g)[d]
Pd/α(N)	0.86	26	4.2	10.9[6]	9.3
Pd/γ(N)	0.77	29	3.9	4.8	134.9
Pd/α(A)	0.65	38	2.9	8.9	8.5
Pd/γ(A)	0.78	60	1.9	2.9	133.2
Pd/ZSM-5	0.90	27	4.1	3.4	272.4
Pd/MCM-22	1.08	25	4.5	4.1	280.0

[a] Pd dispersion, determined from H_2 chemisorption at 100 °C.
[b] Pd particle size, deduced by Eq. (1).
[c] Pd particle size, by TEM.
[d] Specific surface area.

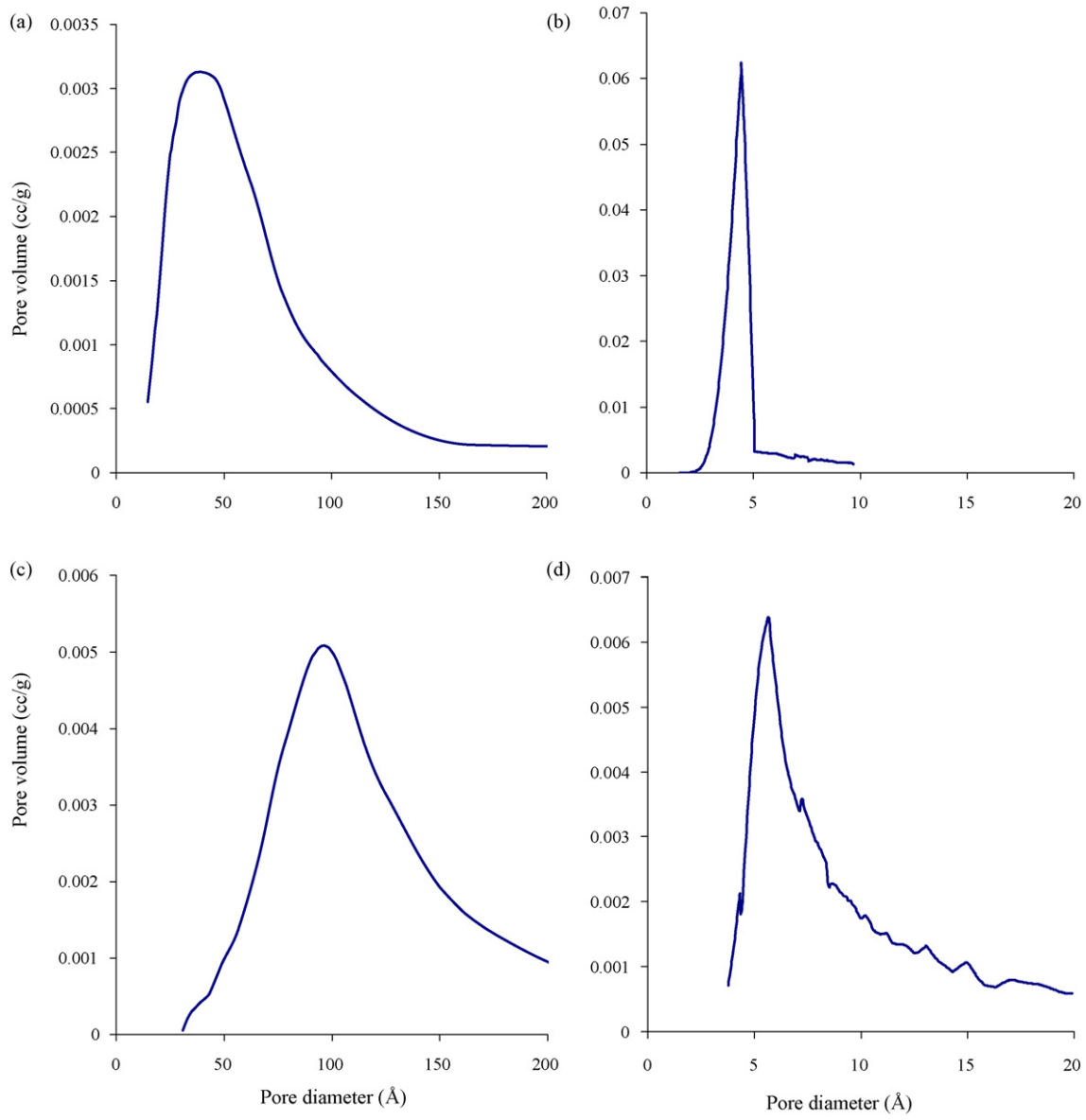

Fig. 2. Pore size distribution. References: (a) Ni–SiO_2, (b) ZSM-5, (c) γ-Al_2O_3, and (d) MCM-22.

interchange, where a covalent bond is created and HAcac is generated ($C_5H_8O_2$), which is adsorbed on the surface [19]. Because the support pre-treatment prior to impregnation with $Pd(acac)_2$ did not promote the dehydroxylation of the surface, the role of the coordinatively unsaturated surface (c.u.s.) aluminum ions for the adsorption of the complex could be excluded [20].

Samples prepared with α- and γ-Al_2O_3 as support did not present differences in their specific area and pore volume with their corresponding supports. In the case of microporous solids, the specific surface area of the catalysts was lower than that of the supports: 272 m^2/g versus 373 m^2/g for Pd-ZSM-5, and 280 m^2/g versus 429 m^2/g for Pd-MCM-22.

XRD patterns of parents MCM-22 and ZSM-5 and their corresponding Pd catalysts are shown in Figs. 3 and 4. In the XRD pattern of the Pd/ZSM-5, all peak positions and intensities matched those reported for the ZSM-5 [21,22] structure, and the same occurred for Pd/MCM-22 [21,23]. The results show that the introduction of Pd particles into MCM-22 and ZSM-5 zeolites did not change the crystal structure of the micropore supports. Furthermore, no characteristic diffractions of crystalline PdOx could be detected in the spectra, indicating the uniform distribution of the particles throughout the matrix of zeolite (its abundance is close to the XRD detection limit).

Table 3 shows palladium dispersion data. When the support was γ-Al_2O_3, the organometallic precursor originated a higher Pd dispersion than the nitrate precursor. Similar results were reported by Vasudevan et al. [24]. When the support was α-Al_2O_3, this behavior was not observed, probably due to the lower surface area of the support and the lack of OH for the acetylacetonate anchoring.

Fig. 5 shows the particle size distribution of the Pd catalysts used in the present study, which were determined from the TEM images for 1000 Pd particles. The distribution is broad for α-Al_2O_3 supported catalyst, and rather narrow for Pd/γ(A). The particle size distribution is an important factor in the analysis of the TPR profile.

The estimation of the Pd particle diameter was performed by TEM micrographs according to the following equation,

$$d_p = \frac{\Sigma_i(n_i d_i^3)}{\Sigma_i(n_i d_i^2)} \quad (1)$$

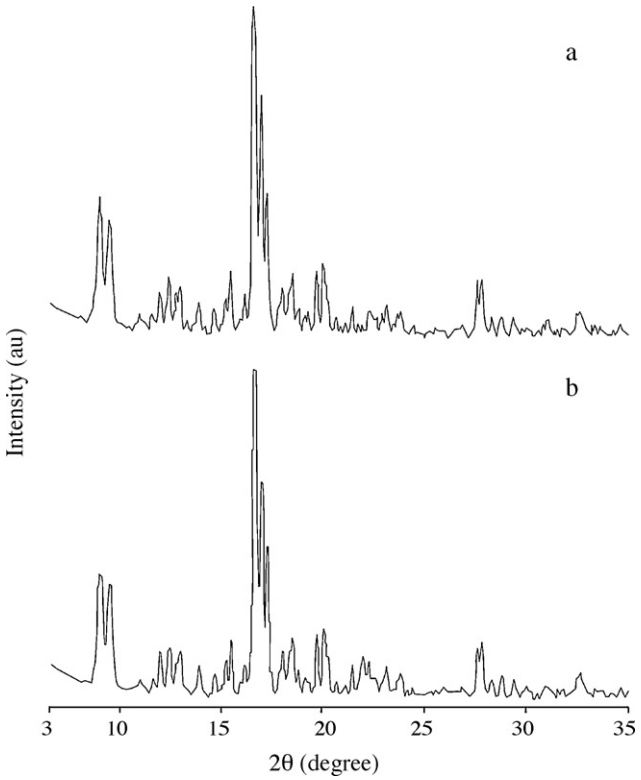

Fig. 3. XRD patterns of parent ZSM-5 (a) and Pd/ZSM-5 catalyst (b).

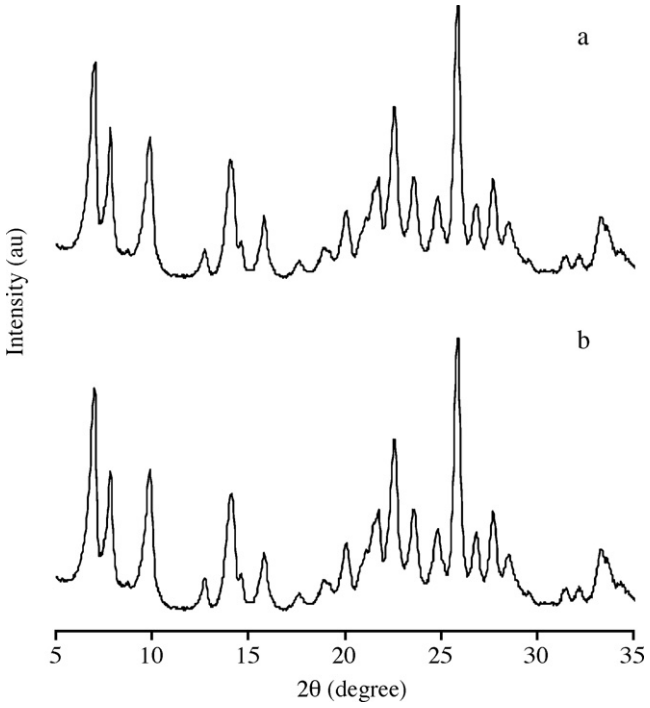

Fig. 4. XRD patterns of parent MCM-22 (a) and Pd/MCM-22 catalyst (b).

and from the H_2 uptake measurements using the following equation,

$$d_p(\text{nm}) = \frac{1,12}{D} \quad (2)$$

where D is the Pd dispersion. It can be observed in Table 3 that the particle sizes obtained by TEM were larger than those calculated by H_2 chemisorption. This could be due to the presence of small particles not detected by the electronic microscope. For samples Pd/ZSM-5 and Pd/MCM-22, it is evident that the majority of the Pd particles (diameter equal to 4.1 and 4.5 nm, respectively) were located in the external surface area of the zeolite (main pore size 4.5 and 5.7 Å). In conclusion, XRD data for the catalysts showed that there was no destruction of the zeolite crystalline structure. On the other hand, the decreased BET surface area and pore volume of

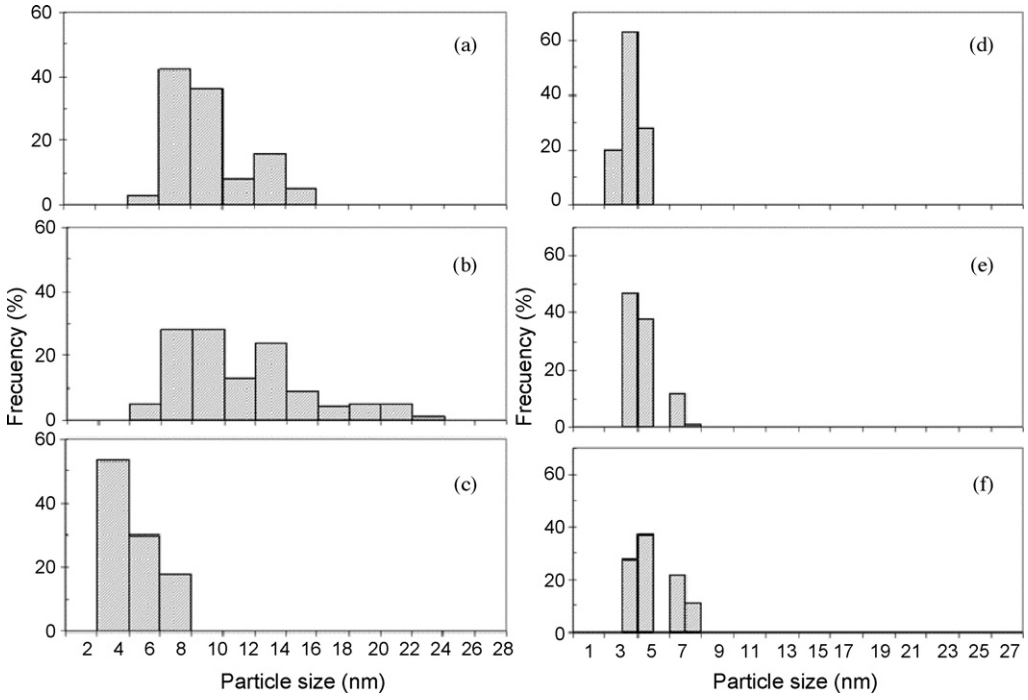

Fig. 5. Particle size distribution determined for1000 PD particles observed by TEM. References: (a) Pd/α(A), (b) Pd/α(N), (c) Pd/γ(N), (d) Pd/γ(A), (e) Pd/ZSM-5, and (f) Pd/MCM-22.

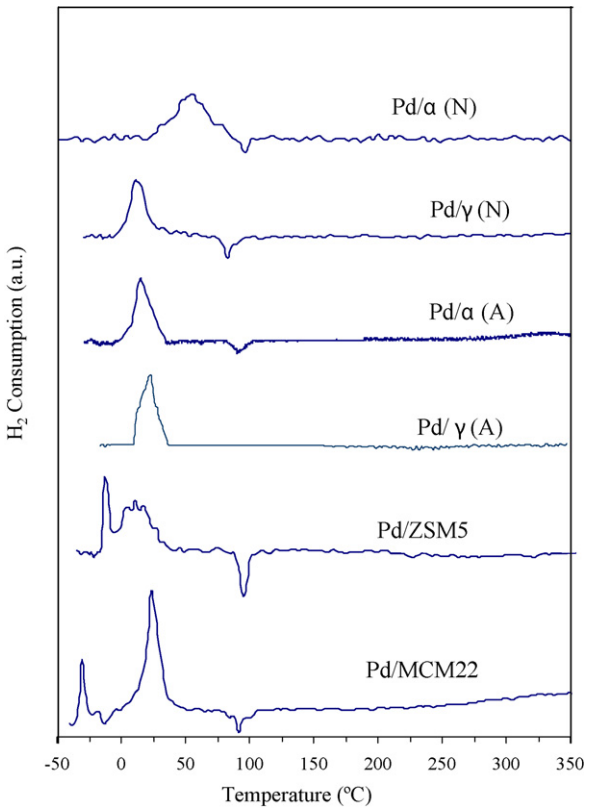

Fig. 6. TPR profile for the studied catalysts. Pre-treatment: oxidation at 300 °C for 1 h.

the Pd catalysts suggest that there was a pore blockage in these catalysts. Pd particle sizes would validate this idea.

Fig. 6 shows the TPR profiles of the calcined samples, where the hydrogen consumption is plotted against temperature. TPR profiles show a positive peak assigned to the reduction of Pd oxide. The negative peak present at 60 °C is attributed to Pd hydride decomposition. Its formation occurs when the catalyst comes into contact with the reducing mixture at low temperature. It is known that Pd hydride is thermodynamically unstable at temperatures above 60 °C. Nevertheless, for supported catalysts, Pd hydride decomposition is affected by the TPR operating conditions, the support nature and the presence of promoters [25].

The Pd hydride decomposition signal was not observed for the Pd/γ(A) sample. This could be due the small average particle size showed by the sample, since the hydride formation is a volumetric phenomenon.

Comparing the two samples supported on α-Al_2O_3, Pd/α(N) and Pd/α(A), different reduction profiles were found: a narrow peak at 25 °C when the precursor used was $Pd(C_5H_7O_2)_2$ and, on the other hand, when the precursor salt was $Pd(NO_3)_2$, the signal was broad at 65 °C. Broad reduction peaks are associated with the presence of particles of various sizes. The latter could be correlated with the particle size distribution of particles obtained by TEM (Fig. 5, a and b).

A similar observation can be made regarding the significant difference in the reduction temperature of PdO in Pd/α(N) and Pd/γ(N) samples (58 and 38 °C, respectively). In this case, the different particle size distribution and the different supports and their interaction with Pd need to be born in mind.

Regarding the zeolite supported catalysts, TPR profiles show two peaks for hydrogen consumption: one very narrow below 0 °C, and the other one wider with a greater area at ~20 °C. Given the characteristics of the support, these profiles could indicate two different particle types: one with a smaller particle size, located inside the zeolite channels (corresponding to the low-temperature consumption peak), including a small fraction of the total due to the small comparative area in the TPR profile, and probably not shown in Fig. 5 because the particle size could be below the detection limit. The other consumption peak would correspond to a larger particle, located in the external surface.

Table 4
Overall reaction constant for the hydrogenation of sunflower oil. Experimental condition: T = 100 °C, P = 413 kPa, agitation rate = 1400 rpm.

Catalyst	ωk_{or} (min^{-1})	k_{or} ($kg_{oil}/min\ g_{metal}$)
Pd/γ(N)	0.0069	0.39
Pd/γ(A)	0.0091	1.09
Pd/α(A)	0.0059	0.38
Pd/α(N)	0.0055	0.40
Pd/ZSM5	0.0072	0.37
Pd/MCM22	0.0114	0.48
Ni[a]	0.0131	0.02

[a] Reaction at 180 °C.

3.2. Catalytic tests

3.2.1. Mass transfer effects

The volumetric gas–liquid mass-transfer coefficient K_La was separately measured using an excess of catalyst load (more than 3%) [16]. The value obtained was in the range 0.3–0.5 s^{-1} and can be considered acceptable [7].

The Weisz–Prater criterion (Eq. (3)) was used to evaluate the intraparticle diffusion limitations:

$$\Phi_I = \frac{(-r_{obs,i})\rho_p R_p^2}{D_{eff,i} C_i} \quad (3)$$

where C_i is the concentration of sunflower oil or H_2 [mol/m^3], D_{eff} the effective diffusion coefficient [m^2/s], R_p indicates the mean particle size [m], $r_{obs,i}$ the observed rate of double bonds or H_2 consumption [$mol/s\ kg_{cat}$], and ρ_p is the apparent density of the catalyst [kg/m^3].

The Weisz–Prater criterion indicates that the mass transfer limitation for the unknown kinetics is negligible when $\Phi_I \ll 1$ [26]. The hydrogen concentration in the liquid was calculated from Andersson et al. [27]. Intraparticle diffusion coefficients for the catalysts were taken as $D_{H_2} = 1.2 \times 10^{-8}\ m^2/s$ and $D_{TAG} = 1 \times 10^{-10}\ m^2/s$ [27]. The density of sunflower oil was determined from [28] as ρ_{TGA} = 0.866 g/ml. The catalyst density was 1574 kg/m^3 for Pd on γ-Al_2O_3, and 2276 kg/m^3 for Pd on α-Al_2O_3. The catalyst particle diameters were 211 and 225 mm for Pd on γ-Al_2O_3 and Pd on α-Al_2O_3, respectively. The tortuousness and porosity values of 4 and 0.5 were adopted. For Ni catalyst, the values were taken from [29].

In the present experiments, the numerical value of the Weisz–Prater modules of H_2 and TAG always remained above 4, indicating that it is not possible to neglect the concentration gradients within the catalyst particle.

3.2.2. Overall catalytic activity

The prepared and characterized catalysts were studied in the partial hydrogenation of sunflower oil at 413 kPa and 100 °C (180 °C for the Ni sample). Following the convention, pseudo-first order rate constants were calculated from IV by assuming that the rate of IV reduction is first order with respect to IV:

$$\frac{d[C{=}C]}{dt} = -\omega k_{or}[C{=}C] \quad (4)$$

where k_{or} is the overall reaction constant at specific reaction conditions, and ω is the ratio = g_{metal}/kg_{oil}.

Table 5
Hydrogenation of sunflower oil: fatty acid composition for IV ≈ 90. Experimental condition: T = 100 °C, P = 413.5 kPa.

Fatty acids (wt%)	Sunflower oil	Partially hydrogenated oil						
		Pd/γ(N)	Pd/γ(A)	Pd/α(A)	Pd/α(N)	Pd/ZSM5	Pd/MCM22	Ni[a]
C16:0	6.1	5.6	5.8	5.69	5.7	4.3	5.3	6.2
C18:0	3.4	5.5	5.6	6.8	6.9	5.5	6.3	9.3
C18:1t	0.0	16.0	14.0	14.2	18.7	14.5	21.6	15.4
C18:1c	35.2	56.3	56.8	55.5	50.2	63.2	53.0	49.2
C18:2t	1.4	5.6	5.9	4.5	3.4	3.5	2.8	2.3
C18:2c	52.6	9.7	10.7	12.1	13.7	8.7	10.1	18.1
C18:3c	0.4	0.1	0.2	0.1	0.1	0.1	0.1	0.0
C20:0	0.1	0.3	0.3	0.3	0.3	0.1	0.2	0.5
C22:0	0.1	0.6	0.7	0.6	0.7	0.1	0.6	0.8
%*trans*	1.4	21.6	18.6	18.7	22.2	18.0	24.3	21.7
S1[b]	–	0.96	0.95	0.92	0.91	1.02	0.96	0.88
S2[c]	–	0.06	0.06	0.10	0.10	0.05	0.07	0.20
$t_{reaction}$ (min)	–	40	20	50	50	40	20	30
IV	124.9	89.1	90.2	89.0	89.4	88.1	86.7	90.9
Catalyst (mg)	–	500	232	483	347	473	480	500

[a] Reaction at 180 °C.
[b] S1 = (C18:1–C18:1_0)/(C18:2_0–C18:2).
[c] S2 = (C18:0–C18:0_0)/(C18:1–C18:1_0).

Table 4 summarizes the k_{or} values for the catalysts studied, which allows to estimate the overall hydrogenation activity. Pd/γ(A) catalyst, with a Pd loading of 0.78 wt% and a 60% dispersion, showed a higher specific activity than the other Pd catalysts. The difference was important, with a value of 1.09 $kg_{oil}/min\ g_{metal}$ for Pd/γ(A) versus 0.38 to 0.48 $kg_{oil}/min\ g_{metal}$ for the other Pd catalysts. Regarding Pd/ZSM5 and Pd/MCM22, in view of what was analyzed in Section 3.1.2, most Pd particles would not be located in the micropores of the samples. Therefore, the microporosity did not affect the activity of the Pd catalysts.

Ni was tested at 180 °C (temperature at which it is used under industrial operating conditions). At this temperature, the k_{or} value for Pd/γ(A) is 7.5 $kg_{oil}/min\ g_{metal}$ (determined with values of Table 5). Thus, the Pd catalyst activity was 375-fold higher than that of the Ni catalyst.

3.2.3. Catalytic activity and selectivity

The hydrogenation of sunflower oil is represented by the variation of the fatty acid content as a function of C=C conversion (and reaction time in a secondary axis) in Figs. 7 and 8. As the present work is focused on the control of *trans*-isomers, the geometrical isomers are examined without taking into account the position of the double bond in the fatty acid chain.

Fig. 7 presents the fatty acid composition for the hydrogenation of sunflower oil carried out over Pd/γ(A) catalyst at 100 °C and 413 kPa. The IV decreased from an initial value of 120.2 to 66.4 (reaction extent: 45%) over the course of 1 h. The linoleic acid (*cis*-C18:2) content decreased from an initial value of 47.0% to 0.9%, whereas the oleic acid (*cis*-C18:1) content increased from 39.6% to 57.2% in 30 min, and then it decreased to 30.0% (1 h reaction time). The stearic acid content remained low at 4–6% for up to 30 min (reaction extent: 27%), and then steadily increased to a final value of 17.5%. The *trans*-C18:1 content increased over the course of the reaction from 0.5% to about 43.7%.

Fig. 8 shows the fatty acid profile when the hydrogenation was carried out over a commercial Ni catalyst. The IV decreased from an initial value of 122.3 to a final value of 58.0 (reaction extent: 55.8%) over the course of 1 h. The *cis*-C18:2 was converted by hydrogenation and isomerization, and its level decreased until total conversion. The levels of oleic acid increased, reaching a maximum value of 50.6% at 40 min (reaction extent: 36.6%) and then decreased to 30.6% after 1 h. The *trans*-C18:1 fatty acid content increased from 0.3% to 32.1% after 60 min. *Trans*-C18:2 showed a different behavior with an increase of up to 2.35% (30 min) followed by a decrease as a result of its hydrogenation (partial or complete). The stearic acid (C18:0) content increased from 3.6 to 29.7% as expected.

Scheme 1 shows the accepted general model for the hydrogenation of sunflower oil, which considers consecutive reactions of the triglyceride saturation together with the *cis*–*trans* isomerization. The concentration of C18:3 fatty acid is very low, and therefore not considered in the scheme. The dashed lines are for negligible reactions. The overall hydrogenation reaction involves the consecutive saturation of *cis*-C18:2 to *cis*-C18:1 and its subsequent saturation to C18:0, as well as the parallel isomerization of *cis*-C18:2 to *trans*-C18:2 and *cis*-C18:1 to *trans*-C18:1. The reaction pathway could also involve the hydrogenation of *trans*-C18:2 to *cis*-C18:1 and *trans*-C18:1 to C18:0.

Pd/γ(A) and Ni catalysts showed a similar overall reaction pathway, but the magnitudes for each reaction step were different. The

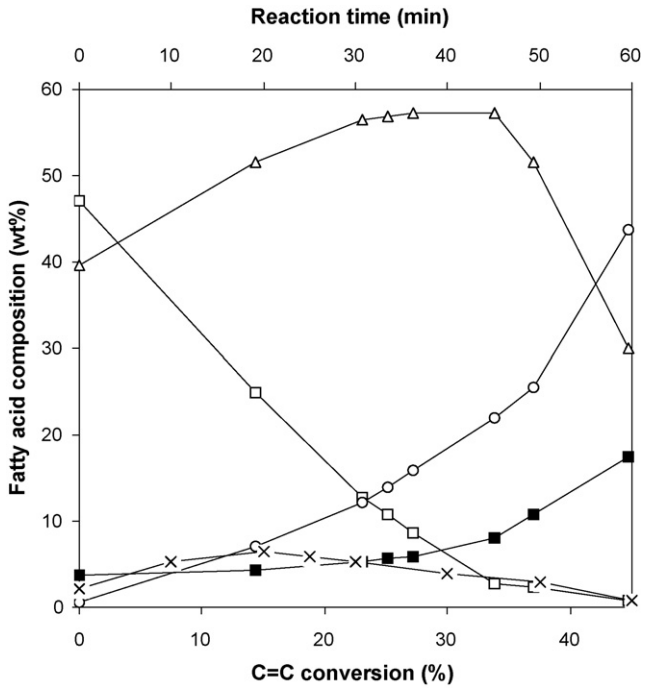

Fig. 7. Fatty acids (%) versus C=C conversion (%) for Pd/γ(A) catalyst (reaction time = 60 min). References: ■, C18:0; △, *cis*-C18:1; ○, *trans*-C18:1; □, *cis*-C18:2; ×, *trans*-C18:2. Operating conditions: 100 °C, 413 kPa, 1400 rpm, catalyst: 232 mg.

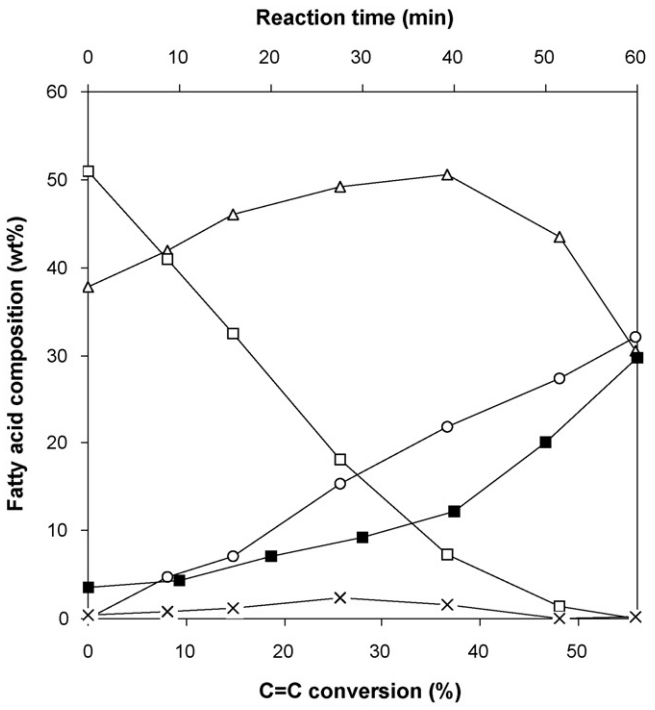

Fig. 8. The fatty acids content as a function of C=C conversion during the sunflower hydrogenation in the presence of the catalysts Ni–SiO_2 (reaction time = 60 min). References: ■, C18:0; △, *cis*-C18:1; ○, *trans*-C18:1; □, *cis*-C18:2; ×, *trans*-C18:2. Operating conditions: 180 °C, 413 kPa, 1400 rpm, catalyst: 500 mg.

saturation of *cis*-C18:1 to C18:0 was more pronounced for the Ni catalyst and lower for the Pd catalyst. The isomerization of *cis*-C18:1 to *trans*-C18:1 was favored by both catalysts, and the isomerization of *cis*-C18:2 to *trans*-C18:2 was higher for Pd catalyst. Nevertheless, Pd/γ(A) generated less *trans*-isomers than the Ni catalyst (18.6% versus 21.7%). That *trans*-isomer concentration is still too high for food application, but Pd/γ(A) is a better catalyst than Ni to produce different base oils for lubricants. The description "Low trans fatty acid content" implies that the product must contain less than 1% *trans* acid, with a normally accepted maximum of 0.8% in the finished product [30].

For all the studied catalysts, the composition of the fatty acids in the partial hydrogenated oil for an IV ≈ 90 is shown in Table 5. In all the cases, there was an increase in the concentration of stearic acid (C18:0) and a decrease in linoleic and linolenic acids (*cis*-C18:2 and *cis*-C18:3) due to the saturation of the double bonds. For the same IV reduction, all the catalysts produced about the same level of *trans*-fatty acid, but Pd catalysts produced less stearic acid and were more selective toward *cis*-C18:1 formation than the Ni catalyst.

Table 5 shows selectivity S1, defined as the amount of monounsaturated fatty acids (C18:1) formed with respect to the amount of diunsaturated fatty acids converted (C18:2), and selectivity S2, defined as the amount of saturated fatty acids (C18:0) produced with respect to the amount of monounsaturated fatty acids (C18:1)

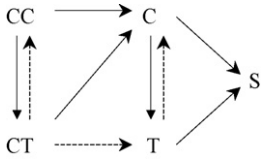

Scheme 1. Hydrogenation–isomerization of sunflower oil. Dashed lines are from negligible reactions. References: CC: *cis*-C18:2, CT: *trans*-C18:2, C: *cis*-C18:1, T: *trans*-C18:1, S: C18:0.

Table 6
TOF (h^{-1}) for Pd/γ(N) and Pd/γ(A) samples.

TOF ($\times 10^3$ h^{-1})		Operating conditions	
Pd/γ(A) d_p[a] = 1.9 nm	Pd/γ(N) d_p = 3.9 nm	T [°C]	P [kPa]
102.5	57.5	120	413
88.2	40.0	100	413
27.5	12.5	80	413
42.5	25.0	100	207
120.0	42.5	100	620

[a] Pd particle size, calculated by Eq. (1).

converted (for IV ≈ 90). The value of S1 was 0.95 and 0.88 for Pd/γ(A) and Ni, respectively. According to these values, Ni produced the lowest level of monounsaturated fatty acids, while the opposite is true for Pd/γ(A). On the other hand, the value of S2 was 0.06 and 0.20 for Pd/γ(A) and Ni, respectively, indicating that the saturation of C18:1 to C18:0 was more pronounced for the Ni catalyst and lower for the Pd catalyst. This tendency was observed for all the Pd catalysts studied in this work.

Pd/γ(A) and Pd/MCM22 presented the highest activity. However, despite its similar activity to Pd/γ(A), the catalyst Pd/MCM22 displayed a high *trans*-fatty acid production (24.3% versus 18.6%).

3.2.4. Influence of the support on the catalytic performance

In this work, four different supports were used in order to study the support effects on the hydrogenation of sunflower oil. Their main properties are listed in Table 2.

Pd/γ(N), Pd/α(A), Pd/ZSM5 and Pd/MCM22 were selected for their similar metallic particle size. In Table 5 it can be observed that MCM-22 supported catalysts were slightly more active than α-Al_2O_3, γ-Al_2O_3 and ZSM5 supported samples. This difference is minor considering the great differences in acidity, pore size distribution and specific surface areas (9.2–429.3 m^2/g) between the selected supports. These results would indicate that the support does not exert an important effect on the hydrogenation of sunflower oil under the selected operating conditions. With respect to the *cis*/*trans* selectivity, Table 4 shows that there is not a significant effect of the support on the *trans*-isomer production.

3.2.5. Effects of Pd particle size

Different precursors were used in order to obtain catalysts with different metallic particle size. The Pd/γ(A) sample presented a smaller particle size than Pd/γ(N), 1.9 nm and 3.9 nm, respectively.

When the catalysts are compared on the basis of their specific activities (k_{or}), the Pd/γ(A) sample was more active exhibiting a specific activity of 1.09 ($kg_{oil}/min\ g_{metal}$), whereas Pd/γ(N) showed a specific activity of 0.39 ($kg_{oil}/min\ g_{metal}$).

Table 6 shows the turn over frequency (TOF, h^{-1}) for different operating conditions. TOF was calculated from the initial rates, which were determined from the slopes. These data suggest that at a smaller particle size, the initial rate is slightly higher. But these differences are small and do not allow to draw a final conclusion. With respect to the *cis*/*trans* selectivity, no significant variations were observed (not shown).

4. Conclusion

Sunflower oil hydrogenation was studied using six palladium catalysts prepared with different precursors and supports (α-Al_2O_3, γ-Al_2O_3, ZSM-5, and MCM-22). A comparative evaluation of the performance of Pd catalysts and a commercial nickel catalyst was carried out.

The samples prepared showed a metal loading in the range 0.7–1 wt% and a main Pd particle size of 2–4.5 nm. In the case of the Pd/ZSM5 and Pd/MCM22 catalysts, most Pd particles were not

located in the micropores of the samples. Therefore, the microporosity did not affect the activity of the catalysts.

Under the studied operating conditions, the different supports did not improve significantly the activity or the selectivity of the reaction. Regarding the effects of Pd particle size, turn over frequency was compared for different operating conditions; the results suggest that at a smaller particle size, the initial rate is slightly higher. But these differences were small and do not allow to draw a final conclusion. With respect to the *cis*/*trans* selectivity, no significant variations were observed.

The γ-alumina supported Pd catalyst, Pd/γ(A), with a metal loading of 0.78 wt% and a 60% dispersion, showed a specific activity higher than the other Pd catalysts, with a value of 1.09 $kg_{oil}/min\,g_{metal}$ versus a 0.38–0.48 $kg_{oil}/min\,g_{metal}$ for the other Pd catalysts. The Pd/γ(A) catalyst activity was 375-fold higher than that of the Ni catalyst (under the same operating conditions).

For the same double bond conversion (IV ≈ 90), this sample originated a slightly lower amount of total *trans*-isomers than the Ni catalyst (18.6% versus 21.7%). The value of S1 was 0.95 and 0.88 for Pd/γ(A) and Ni, respectively. According to these values, Ni produced the lowest level of monounsaturated fatty acids, while the opposite was true for Pd/γ(A). On the other hand, the value of S2 was 0.06 and 0.20 for Pd/γ(A) and Ni, respectively, indicating that the saturation of C18:1 to C18:0 was more pronounced for the Ni catalyst and lower for the Pd catalyst. This tendency was observed for all the Pd catalysts studied in this work. The *trans*-isomer concentration is still too high for food application, but Pd/γ(A) is a better catalyst than Ni to produce base oils for lubricants.

Acknowledgements

The authors thank the *Agencia Nacional de Promoción Científica y Tecnológica* (National Agency of Scientific and Technological Promotion, Argentina) and the *Consejo Nacional de Investigaciones Científicas y Técnicas* (National Council for Scientific and Technological Research (CONICET)) for the financial support.

References

[1] J. Coenen, Hydrogenation of edible oils, J. Am. Oil Chem. Soc. 53 (1976) 382–389.
[2] D. Mozaffarian, E. Rimm, I. King, R. Lawler, G. McDonald, W. Levy, *Trans* fatty acids and systemic inflammation in heart failure, Am. J. Clin. Nut. 80 (2004) 1521–1525.
[3] S. Han, L. Leka, A. Lichtenstein, L. Ausman, E. Schaefer, S. Meydani, Effect of hydrogenated and saturated, relative to polyunsaturated, fat on immune and inflammatory responses of adults with moderate hypercholesterolemia, J. Lipid Res. 43 (2002) 445–452.
[4] K.-W. Lee, B. Mei, Q. Bo, Y.-W. Kim, K.-W. Chung, Y. Han, Catalytic selective hydrogenation of soybean oil for industrial intermediates, J. Ind. Eng. Chem. 13 (2007) 530–536.
[5] B. Nohair, C. Especel, G. Lafaye, P. Marecot, L.C. Hoang, J. Barbier, Palladium supported catalysts for the selective hydrogenation of sunflower oil, J. Mol. Catal. A 229 (2005) 117–126.
[6] J. Ray, Behavior of hydrogenation catalysts. I. Hydrogenation of soybean oil with palladium, J. Am. Oil Chem. Soc. 62 (1985) 1213–1217.
[7] E. Santacesaria, P. Parrella, M. Di Sergio, G. Borrelli, Role of mass transfer and kinetics in the hydrogenation of rapeseed oil on a supported palladium catalyst, Appl. Catal. A 116 (1994) 269–294.
[8] M. Plourde, K. Belkacemi, J. Arul, Hydrogenation of sunflower oil with novel catalysts supported on structured silica, Ind. Eng. Chem. Res. 43 (2004) 2382–2390.
[9] M. Fernández, C. Piqueras, G. Tonetto, G. Crapiste, D. Damiani, Hydrogenation of edible oil over Pd–Me/Al_2O_3 catalysts (Me = Mo, V and Pb), J. Mol. Catal. A 233 (2005) 133–139.
[10] M. Fernández, G. Tonetto, G. Crapiste, M. Ferreira, D. Damiani, Hydrogenation of edible oil over Pd catalysts: a combined theoretical and experimental study, J. Mol. Catal. A 237 (2005) 67–79.
[11] G. Leofanti, M. Padovan, G. Tozzola, B. Venturelli, Surface area and pore texture of catalysts, Catal. Today 41 (1998) 207–219.
[12] G. Horvath, K. Kawazoe, Method for the calculation of effective pore size distribution in molecular sieve carbon, J. Chem. Eng. Jpn. 16 (1983) 470–475.
[13] L. Cheng, R. Yang, Improved Horvath–Kawazoe equations including spherical pore models for calculating micropore size distribution, Chem. Eng. Sci. 49 (1994) 2599–2609.
[14] L. Konopny, A. Juan, D. Damiani, Preparation and characterization of γ-Al_2O_3-supported PdMo catalysts, Appl. Catal. B 15 (1998) 115–127.
[15] G. Tonetto, D. Damiani, Performance of Pd–Mo/γ-Al_2O_3 catalysts for the selective reduction of NO by methane, J. Mol. Catal. A 202 (2003) 289–303.
[16] O. Stenberg, N.-H. Schöön, Aspects of the graphical determination of the volumetric mass-transfer coefficient (k_La) in liquid-phase hydrogenation in a slurry reactor, Chem. Eng. Sci. 40 (1985) 2311–2319.
[17] P. Weisz, D. Prater, Interpretation of measurements in experimental catalysis, Adv. Catal. 6 (1954) 143–196.
[18] S. Brunauer, L. Deming, E. Deming, E. Teller, On a theory of the van der Waals adsorption of gases, J. Am. Chem. Soc. 62 (1940) 1723–1732.
[19] E. Lesage-Rosenberg, G. Vlaic, H. Dexpert, P. Lagarde, E. Freund, Exafs analysis of low-loaded palladium on alumina catalysts, Appl. Catal. 22 (1986) 211.
[20] M. Womes, J. Lynch, D. Bazin, F. Le Peltier, S. Morin, B. Didillon, Interaction between Pt(acac)$_2$ and alumina surfaces studied by XAS, Catal. Lett. 85 (2003) 25.
[21] M.M.J. Treacy, J.B. Higgins, R. von Ballmoos, Collection of Simulated XRD Powder Patterns for Zeolites, 3rd ed., Elsevier, Amsterdam, 1996.
[22] T. Hardenberg, L. Mertens, P. Mesman, H.C. Muller, C.P. Nicolaides, Zeolites 12 (1992) 685.
[23] L.S. Marques, J.L.F. Monteiro, H.O. Pastore, Micropor. Mesopor. Mater. 32 (1999) 131.
[24] S. Vasudevan, J. Cosyns, E. Lesage, E. Freund, H. Dexpert, Preparation of Catalysts III, vol. 463, Jacobs Editors, 1983.
[25] R. Nandi, P. Georgopoulos, J. Cohen, J. Butt, R. Burwell Jr., D. Bilderback, Pd/SiO_2. II. Effects of pretreatment on structure, J. Catal. 77 (1982) 421–431.
[26] H. Fogler, L. Scott, Elements of Chemical Reaction Engineering, 3rd ed., Prentice Hall, New Jersey, 1999.
[27] K. Andersson, M. Hell, L. Löwendahl, N.-H. Schöön, Diffusivities of hydrogen and glyceryl trioleate in cottonseed oil at elevated temperature, J. Am. Oil Chem. Soc. 51 (1974) 171–173.
[28] D. Swern (Ed.), Bailey's Industrial Oil and Fat Products, vol. 2, 4th edition, 1982.
[29] M. Fernández, G. Tonetto, G. Crapiste, D. Damiani, Revisiting the hydrogenation of sunflower oil over a Ni catalyst, J. Food Eng. 82 (2007) 199–208.
[30] R. Cook, Thermally induced isomerism by deodorization, INFORM 13 (2002) 71–76.